International Journal of Chronic Obstructive Pulmonary Disease

Dovepress
Taylor & Francis Group

Open Access Full Text Article

ORIGINAL RESEARCH

Exploring the Mechanisms of Lijin Fang on Treg/Th17 Cell Imbalance in COPD Based on Network Pharmacology

Zhan-Hua Li[1,*], Si-Ning Chen[1,*], Ling Pan[1,*], Rui Liu[1], Wei Liang[1], Mei-Qun Luo[1], Hai-fei Liao[1], Jie Feng[1], Hao-Zhou Wang[1], Yue-Gan Huang[1], Jing-Hui Zheng[2]

[1]Department of Respiratory and Critical Care Medicine, Ruikang Hospital Affiliated to Guangxi University of Chinese Medicine, Nanning, Guangxi, People's Republic of China; [2]Academic Affairs Office, Guangxi University of Chinese Medicine, Nanning, Guangxi, People's Republic of China

*These authors contributed equally to this work

Correspondence: Zhan-Hua Li, Ruikang Hospital Affiliated to Guangxi University of Chinese Medicine, Nanning, Guangxi, People's Republic of China, Email lizhanhua2024@stu.gxtcmu.edu.cn; Jing-Hui Zheng, Guangxi University of Chinese Medicine, Nanning, Guangxi, People's Republic of China, Email jinghuizheng@yeah.net

Background: Chronic Obstructive Pulmonary Disease (COPD) is chronic respiratory disease that severely affects patients' quality of life and is associated with high mortality rates. Investigating the imbalance between regulatory T cells (Tregs) and T helper 17 cells (Th17) in COPD treatment is crucial, as this imbalance plays a significant role in the disease's inflammatory processes. This study explores the therapeutic potential of the traditional Chinese medicine(TCM) formula, Lijin Fang (LJF), focusing on its ability to restore Treg/Th17 balance.

Methods: We employed bioinformatics and in vitro cell experiments to analyze the active components and targets of LJF. Network pharmacology, differential gene expression, pathway enrichment, ROC model prediction, and immune infiltration analyses were conducted, followed by molecular docking studies. Rat peripheral blood mononuclear cells (PBMCs) were cultured and treated with cigarette smoke extract (CSE) and LJF-containing serum, with flow cytometry, ELISA, and Western blotting used to assess relevant markers.

Results: Our findings demonstrate that treatment with (10% or 30%)LJF-containing serum significantly increased the proportion of Treg cells while concurrently decreasing Th17 cell populations in the 5%CSE-treated rat PBMC model ($p<0.001$). We observed a reduction in pro-inflammatory cytokines such as interleukin-17 (IL-17), tumor necrosis factor-alpha (TNF-α), and interleukin-1 beta (IL-1β), alongside an increase in the anti-inflammatory cytokine interleukin-10 (IL-10) ($p<0.001$). Additionally, potential therapeutic targets, including IL-10, potassium voltage-gated channel subfamily N member 4 (KCNN4), and Baculoviral IAP repeat-containing protein 3 (BIRC3), were identified. Molecular docking results indicated stable interactions between IL-10 and BIRC3 with the constituents of LJF.

Conclusion: This study highlights LJF's anti-inflammatory potential in restoring the Treg/Th17 balance and regulating cytokine expression in COPD.

Keywords: COPD, LJF, Treg/Th17, network pharmacology

Introduction

Chronic Obstructive Pulmonary Disease (COPD) is a progressive respiratory condition characterized by persistent airflow limitation. The disease significantly impairs patients' quality of life and imposes a substantial economic burden on healthcare systems globally.[1,2] Approximately 100 million individuals in China are affected by COPD, with a prevalence of 8.6% among adults aged 20 and older, 13.7% among those aged 40 and above, and exceeding 27% in individuals aged 60 and older. COPD, the third most common chronic disease in China imposing a heavy economic burden, is projected to cause a global economic loss of US$4.326 trillion between 2020 and 2050, with China bearing the

Received: 6 January 2025
Accepted: 7 June 2025
Published: 5 July 2025

largest burden of US$1.363 trillion.[3,4] Current COPD therapies primarily consist of pharmacological interventions, such as bronchodilators and corticosteroids, along with supplemental oxygen. However, these approaches are limited in halting disease progression and often inadequately relieve symptoms or improve overall patient well-being.[2] Consequently, there is a pressing need for innovative therapeutic approaches that can address these limitations and improve patient outcomes.

Traditional Chinese Medicine (TCM) has been utilized in China for thousands of years, accumulating a wealth of clinical experience and demonstrating clear advantages in the treatment of COPD.[5] The modified prescription of Lijin Fang (LJF), composed of thirteen traditional Chinese herbs, is widely applied in the treatment of patients with Lung Qi Deficiency Syndrome during the stable phase of COPD at the Department of Respiratory and Critical Care Medicine of the Affiliated Ruikang Hospital, Guangxi University of Chinese Medicine. Preliminary studies have shown that basic formula of LJF can reverse the increased ratio of Th17 cells to CD4+ T cells induced by cigarette smoke extract(CSE), and its potential mechanism may be related to the inhibition of the JAK2-STAT3-ROR-γt pathway;[6] however, the specific mechanism by which Lijinfang regulates Treg/Th17 remains not fully elucidated. This study uniquely focuses on the therapeutic potential of the TCM compound LJF in the management of COPD, particularly through its modulation of the Treg/Th17 immune cell balance. Previous research has established the critical roles of Treg and Th17 cells in the pathogenesis of COPD, with an imbalance between these cell types contributing to the inflammatory processes underlying the disease.[7]

Traditional Chinese Medicine (TCM) has been utilized in China for thousands of years, accumulating a wealth of clinical experience and demonstrating clear advantages in the treatment of COPD.[5] The modified prescription of Lijin Fang (LJF), composed of thirteen traditional Chinese herbs, is widely applied in the treatment of patients with Lung Qi Deficiency Syndrome during the stable phase of COPD at the Department of Respiratory and Critical Care Medicine of the Affiliated Ruikang Hospital, Guangxi University of Chinese Medicine. Preliminary studies have shown that basic formula of LJF can reverse the increased ratio of Th17 cells to CD4+ T cells induced by cigarette smoke extract(CSE), and its potential mechanism may be related to the inhibition of the JAK2-STAT3-ROR-γt pathway;[6] however, the specific mechanism by which Lijinfang regulates Treg/Th17 remains not fully elucidated. This study uniquely focuses on the therapeutic potential of the TCM compound LJF in the management of COPD, particularly through its modulation of the Treg/Th17 immune cell balance. Previous research has established the critical roles of Treg and Th17 cells in the pathogenesis of COPD, with an imbalance between these cell types contributing to the inflammatory processes underlying the disease.[7]

This study employs network pharmacology and bioinformatics approaches, along with in vitro experimental validation, to investigate the effects of the TCM compound LJF on COPD. Network pharmacology integrates various technologies, including systems biology and bioinformatics, and combines multidimensional information related to "TCM components-targets-diseases", which aligns well with the characteristics of TCM that involves multiple components, multiple targets, and multiple mechanisms of action.[8] Research in network pharmacology is conducive to constructing "compound-gene-disease" networks and revealing the regulatory mechanisms of small molecules. This approach provides a scientific methodology for the study of TCM formulas, enhancing the technological standards of TCM research.[9] In network pharmacology studies, receiver operating characteristic (ROC) curves can be used to evaluate the efficacy of specific targets in diagnosing or predicting diseases, helping determine their clinical applicability by analyzing sensitivity and specificity. Additionally, immune infiltration analysis assesses the infiltration of various immune cells in tissues post-treatment with TCM formulations. By examining changes in the proportions and functional states of immune cells, we can elucidate how TCM formulations exert immunomodulatory effects through the regulation of immune cell recruitment, activation, and immune factor secretion.COPD is a dynamic pathological process involving various cells and mechanisms, and employing network pharmacology strategies can effectively elucidate the multiple effects of TCM formulas in this context.

The advantage of this study lies in its ability to systematically analyze the active components of LJF and their corresponding molecular targets, thereby elucidating the underlying mechanisms of action. By integrating network pharmacology, differential gene expression analysis, pathway enrichment analysis, ROC modeling, and immune infiltration analysis, this study aims to provide a robust theoretical foundation for the clinical application of LJF. Furthermore,

the study includes the cultivation of rat peripheral blood mononuclear cells (PBMCs) exposed to CSE and treated with LJF, followed by flow cytometry, ELISA, and Western blotting (WB) to assess relevant biomarkers. Ultimately, the objective of this study is to uncover the potential therapeutic mechanisms of LJF in the context of COPD. This study provides a new theoretical foundation for the application of TCM formulations in the treatment of COPD through the regulation of Treg/Th17, while also opening up new avenues for therapeutic strategies against COPD.

Materials and Methods

Screening of Active Ingredients and Targets of LJF

SymMap, TCMID, TCMSP, and TCM-ID are four significant databases related to TCM, each providing important information regarding TCM substances, their components, mechanisms, and applications.The active components of the TCM LJF, which consists of Ren Shen (Ginseng), Huang Qi (Astragalus), Mai Dong (Ophiopogon), Wu Wei Zi (Schisandra), Zi Wan (Aster), Chuan Bei Mu (Fritillaria), Tu Si Zi (Cuscuta), Bai Zhu (Atractylodes), Fang Feng (Saposhnikovia), Fu Ling (Wolfiporia cocos), Chen Pi (Dried Tangerine Peel), Gan Cao (Licorice), and Yin Yang Huo (Epimedium brevicornu), were obtained from the SymMap(http://www.symmap.org/), TCM Integrated Database (TCMID, http://www.megabionet.org/tcmid/), TCM Systems Pharmacology Database and Analysis Platform (https://old.tcmsp-e.com/tcmsp.php,TCMSP), and TCM Information Database (TCM-ID, https://www.bidd.group/TCMID/) databases. The aforementioned datasets are currently widely used systems pharmacology platforms that provide valuable support for the in-depth study of the essence of TCM theory, the revelation of the mechanisms of action of TCM, and the development of novel TCM-oriented drugs.[10,11] The corresponding target proteins for these components were identified using the aforementioned databases. The gene names of the targets were then validated and corrected using the UniProt database (https://www.uniprot.org/). Subsequently, an interaction network model illustrating the interactions between LJF, its active components, and their potential targets was constructed using Cytoscape 3.7.2 software (https://cytoscape.org/).

Acquisition of Disease Targets

The Gene Expression Omnibus (GEO) is a public database maintained by the National Center for Biotechnology Information (NCBI) that is specifically designed for storing high-throughput gene expression data and other functional genomics data.Transcriptional chip data related to “Chronic Obstructive Pulmonary Disease (COPD)” were downloaded from the GEO database (https://www.ncbi.nlm.nih.gov/geo/) with the following screening criteria: ① the keyword “Chronic Obstructive Pulmonary Disease”; ② species limited to humans. The chip data were corrected for background, normalized, and expression values were calculated using the Bioconductor R package within R. Using Perl scripts and the R SVA package for annotation and batch correction of the raw data, differential analysis was performed with the DESeq2 and limma packages to compute differentially expressed mRNAs between the two groups, with the criteria for selecting differentially expressed genes set to a P value of <0.05 and a fold change of ≥ 2.00 ($|\log2 FC| \geq 1.00$). Here, $\log2FC \geq 1.00$ indicates upregulated mRNA expression, while $\log2FC \leq -1.00$ indicates downregulated mRNA expression.The adjusted p-values (padj) returned by the DESeq2 package were utilized for multiple testing correction, which were calculated using the Benjamini-Hochberg method to control the False Discovery Rate (FDR).As a result, the differentially expressed mRNAs in “COPD” referred to as Different Expressed Genes (DEGs), were identified. The heatmap package was utilized to generate heat maps and perform cluster analysis of the selected DEGs. The P values from the differential analysis were transformed using -log10, and the results were classified according to the log2FC into three groups (upregulated DEGs, downregulated DEGs, and DEGs with no statistical significance). The processed data were then imported into R for the generation of a volcano plot. Furthermore, gene set enrichment analysis (GSEA) was conducted using the clusterProfiler R package on the gene sets from the COPD dataset, focusing on the “hallmark gene sets” to explore the biological functions between the gene sets of COPD and normal tissues.

Establishment of Expression Matrix for Treg/Th17 Immune Cell-Related Genes in COPD

Combine the previously obtained mRNA expression matrix of COPD with the 542 Treg/Th17 immune cell-related genes to form a comprehensive expression matrix. The limma R package was then employed to identify differentially expressed genes associated with Treg/Th17 immune cells (IMM-DEGs) between the COPD group and the healthy control group. The selection criteria were as follows: a corrected P value < 0.05. This process resulted in the identification of Treg/Th17 immune cell-related differentially expressed mRNAs in COPD. The pheatmap packages were utilized to visualize the selected DEGs using heatmap. Statistical comparisons of gene expression between the COPD and control groups were conducted, with a P value < 0.05 considered statistically significant.

Relative Expression Levels of Core Targets and ROC Evaluation

The targets of the active pharmaceutical ingredients obtained in the preliminary phase were imported into the online Venn diagram generation tool, InteractiVenn, together with the previously identified IMM-DEGs, to match and map potential core targets. Based on the core targets identified in the previous steps, the ggpubr package was utilized to analyze the relative expression levels of these core targets within the COPD expression data, and box plots were generated to illustrate their relative expression. The normalized expression data of COPD core targets were then merged with clinical data for COPD patients. The R packages pROC, and ggplot2 were employed to plot ROC curves for the core genes associated with COPD.

Immune Infiltration Analysis of Core Targets Related to COPD

The expression matrix data pertaining to COPD was analyzed using the CIBERSORT package to perform deconvolution algorithms. This approach estimates the cellular composition of complex tissues based on normalized gene expression data and quantifies the abundance of specific cell types.[12] The resulting expression matrix of infiltrating immune cells associated with COPD was generated, and immune cell sorting was performed using Perl scripts for immune selection. The limma R package was employed to conduct background correction, normalization, and expression value calculations for the chip data, and the CIBERSORT package was utilized to estimate the immune cell composition in COPD. Furthermore, the CIBERSORT package was used to analyze the composition of immune cells in each sample, followed by the creation of bar plots to visualize the data. Subsequently, the corrplot package was employed to analyze the interactions between different immune cell populations in COPD, with the creation of co-expression plots for immune cell infiltration.

Gene Ontology (GO) Biological Function Analysis and KEGG Pathway Enrichment

The clusterProfilerGO.R package in R software (https://www.r-project.org/) and Perl language were employed to conduct GO analysis on the immune-related common targets of LJF and "COPD". GO analysis is primarily used to describe the functions of gene products, which includes three main aspects: Cellular Component (CC), Molecular Function (MF), and Biological Process (BP).[13] Additionally, the clusterProfiler KEGG.R package was utilized for KEGG pathway enrichment analysis, complemented by the pathview package to create corresponding pathway diagrams. The degree of pathway enrichment was assessed based on enrichment factor values, in order to explore the potential biological functions and signaling pathway mechanisms by which LJF may exert therapeutic effects on COPD.

Screening of TCM Components

Virtual screening through docking provides appropriate indications of the potential biological activities of compounds, reducing the cost and time of drug discovery.[14] The active ingredients of LJF were screened based on oral bioavailability (OB) ≥ 30% and drug-likeness (DL) ≥ 0.18, with molecular structures downloaded in mol*2 format from the PubMed database. The core protein domain structures in pdb format were obtained from the PDB database (http://www.rcsb.org/). Virtual screening was performed using the Libdock module of Discovery Studio 2019. The specific operations included: clearing water molecules from the receptor protein, and energy minimization of the protein-ligand complex using

DS2019. For the accurate ionization of amino acid residues and tautomeric states, all non-polar hydrogens were merged, and partial atomic charges were assigned using the Gasteiger-Marsili method. Further molecular docking was conducted to assess the potential binding modes between the active ingredients from the TCMSP drug database and the binding sites of the core protein. The top three compounds with the highest LibDockScore values were selected for subsequent calculations of binding energy and RMSD values. The specific procedures involved using PyMOL software to remove water and phosphate groups from the protein, and AutoDockTools 1.5.7 software was employed to convert the pdb format files of the three active ingredients and core protein gene files into pdbqt format, while identifying the active pockets. Finally, the Vina script was executed to calculate molecular binding energies and display the docking results. The molecular docking results of the ligand-receptor complex were presented in both 3D and 2D formats to evaluate the reliability of the predictions made through bioinformatics analysis.

Preparation of Cigarette Smoke Extract (CSE)

Following the method described by Li and making improvements,[15] In a 75 mL conical tube, 20 mL of RPMI 1640 culture medium was added as the absorption liquid. One end of the tube was connected to a cigarette (Double Happiness brand, produced by Guangdong Tobacco Industry Co., Ltd., with a tar content of 11 mg, nicotine content of 1.2 mg, and carbon monoxide content of 11 mg), while the other end was attached to a 50 mL syringe. After igniting the cigarette, the number of puffs taken per cigarette was controlled at 15, and smoke was drawn at a steady rate until the cigarette was completely consumed. The glass bottle was shaken to ensure complete dissolution of the smoke. The collected liquid was transferred to a centrifuge tube, filtered, and its pH was adjusted to 7.2. The optical density (OD) values measured at 450 nm were equal to 1, indicating a 100% CSE stock solution. The stock solution was then aliquoted and stored at −80°C. Prior to use, it was diluted with an appropriate volume of culture medium, and the prepared CSE at various concentrations was used within 30 minutes.

Preparation of Drug-Containing Serum

LJF (composed of ginseng, astragalus, ophiopogon, schisandra, aster, fritillaria, dodder, Atractylodes, Wolfiporia cocos, saposhnikovia, dried tangerine peel, licorice, and Epimedium brevicornu) was provided by the Pharmacy Department of the Affiliated Ruikang Hospital of Guangxi University of Chinese Medicine. All components of the LJF were products from Guangxi Xianzhujiao TCM Technology Co., Ltd., with the following production batch numbers: ginseng (P221216); astragalus (P230308); ophiopogon (P221247); schisandra (2308176–1); aster (P220290); Wolfiporia cocos (P220740); Atractylodes (P230238); saposhnikovia (P230420); dried tangerine peel (P230538); licorice tablets (P230028); fritillaria (P20240101); Epimedium brevicornu (P221562); dodder (P220834). Prepare the LJF by dissolving it in physiological saline prior to the experiment.

Six 7-week-old male SD rats (Guangzhou Ruige Biotechnology Co., Ltd., Batch No. 44827200011597, animal experiment approval number: DW20240603-151) were divided into control group and drug group (N=3 rats/group). The drug group received LJF at a dosage of 4.48 g per rat per day, while the control group was administered an equivalent volume of saline. After continuous gavage for 7 days, inhalation anesthesia was performed using 4% isoflurane prior to blood collection, blood was collected from the abdominal aorta. The blood samples were centrifuged at 1500g for 10 minutes to obtain serum, which was then aliquoted and stored at −20°C for future use.[16,17]

Solution of PBMCs from Rats

Blood was collected from the abdominal aorta of 7-week-old male SD rats. The blood was mixed with PBS (Biosharp BL302A, USA) at a 1:1 ratio, and an appropriate amount of Ficoll (YEASEN 40502ES25, China) density gradient medium was added to a centrifuge tube. The diluted blood was then layered on top of the Ficoll solution. Using a centrifuge (Hema TGL-16R, China), the samples were centrifuged at approximately 400 g for 30 minutes. After centrifugation, the PBMC layer was located between the plasma layer and the Ficoll layer, and this layer was carefully collected. The PBMCs were then seeded into culture flasks and cultured with complete RPMI 1640 medium (Gibco 11875–093, USA) supplemented with 10% FBS (Gibco 16000–044, USA) and 1% penicillin-streptomycin mixed solution (Biosharp BL505A, USA) in a 37°C, 5% CO2 incubator for subsequent experiments.

Screening for the Optimal Concentration of CSE

A total of 5×10^5 rat PBMCs were seeded into each well of a 6-well culture plate using complete RPMI 1640 medium and incubated overnight in a 37°C, 5% CO2 incubator to achieve 70–90% confluence by the following day. The cells were treated with different concentrations of CSE (1%, 5%, 10%, and 30%) for 48 hours. Subsequently, flow cytometry was performed to detect Treg (CD3+CD4+FOXP3+) and Th17 (CD3+CD4+IL17) cell populations. The appropriate concentration of CSE was selected for subsequent experiments.

Cell Experiment and Grouping

A total of 5×10^5 rat PBMCs were seeded into each well of a 6-well culture plate using complete RPMI 1640 medium and incubated overnight in a 37°C, 5% CO2 incubator to achieve 70–90% confluence the following day. The PBMCs were then randomly divided into the following groups:

1. Control group (normal culture),
2. CSE group (5% CSE + blank serum, treated for 48 hours).
3. CSE + LJF low concentration group (5% CSE + 10% drug-containing serum from LJF, treated for 48 hours).
4. CSE + LJF high concentration group (5% CSE + 30% drug-containing serum from LJF, treated for 48 hours).

Flow Cytometry Detection

Cell suspensions from each group were collected and resuspended in PBS. A total of 100 μL of 3% BSA (Biosharp BS114, USA) was added to resuspend the cells into a single-cell suspension and incubated at room temperature for 15 minutes for blocking. Following the manufacturer's instructions, the appropriate volumes of antibodies against CD3 (E-AB-F1228J, Elabscience, China), CD4 (E-AB-F1105C, Elabscience, China), FOXP3 (B369751, BioLegend, China), and IL-17 (17–7177-81, eBioscience, USA) were added and mixed thoroughly. The mixture was then incubated in the dark at room temperature for 30 minutes.

After incubation, the cells were centrifuged at 300 g for 5 minutes, and the supernatant was discarded while retaining the cell pellet. The cells were resuspended in 500 μL of PBS and analyzed using a flow cytometer (BD FACSCanto™ II Flow Cytometer, USA). Data analysis was performed using FlowJo software.

The gating strategy consists of four steps: First, lymphocytes are identified based on forward scatter (FSC) and side scatter (SSC) characteristics, excluding debris, dead cells, and non-lymphocyte components. Second, $CD3^+$ T cells are identified within the lymphocyte population, and $CD4^+$ T cell subsets are further distinguished based on CD4 expression. Next, within the $CD4^+$ T cell subset, Treg cells are identified by FOXP3 expression, while Th17 cells are identified based on IL17 expression. Control settings include isotype controls to exclude non-specific background fluorescence, unstimulated controls to assess natural background expression levels, and unstained controls to differentiate between spontaneous autofluorescence and specific fluorescence.

ELISA Detection

Cells from each group were collected and washed with pre-cold PBS. The cells were subjected to repeated freeze-thaw cycles to facilitate lysis. The resulting extract was centrifuged at 1500 g for 10 minutes, and the supernatant was collected. Following the instructions provided in the ELISA kits, the levels of the following cytokines were measured:Rat Interleukin 1β (IL-1β) ELISA Kit (RUIXIN BIOTECH RX2D302066, China),Rat Tumor Necrosis Factor α(TNF-α) ELISA Kit (RUIXIN BIOTECH RX2D310636, China),Rat Interleukin 17 (IL-17) ELISA Kit (RUIXIN BIOTECH RX302873R, China),Rat Interleukin 10 (IL-10) ELISA Kit (RUIXIN BIOTECH RX302880R, China).Measurements were performed according to the manufacturer's protocols.

Western Blotting Detection

Proteins from each group of cells were extracted and quantified. Subsequently, the target proteins were analyzed using a 12% polyacrylamide gel. Following SDS-PAGE electrophoresis, the proteins were transferred to a PVDF membrane (ISEQ00010, MerckMillipore, USA). After blocking with 5% BSA (blocking buffer, Japan), the membrane was

incubated overnight at 4°C with the following primary antibodies: KCNN4 (1:1000, YP-AB16315, Youpin Bioscience, China), IL-10 (1:2000, 60269-1-ig, Proteintech, USA), cIAP2/BIRC3 (1:500, A0833, ABCLONAL, China), and GAPDH (1:50000, 60004-1-Ig, Proteintech, USA).

Data Statistical Analysis

In this study, statistical analysis was conducted using SPSS 26.0 (IBM, USA). Measured data are presented as mean ±standard deviation. Normality tests and homogeneity of variance tests were performed. Comparisons between two groups were conducted using an unpaired *t*-test. Comparisons among groups were analyzed using one-way analysis of variance (ANOVA). A p-value <0.05 was considered statistically significant.

Results

Active Ingredients and Corresponding Targets of the Drug

A search through the SymMap, TCMID, TCMSP, and TCM-ID databases, followed by screening based on ADME principles, identified a total of 2048 active ingredients in LJF. These included 418 from Ginseng, 167 from Astragalus, 55 from Ophiopogon, 171 from Schisandra, 95 from Aster Tataricus, 166 from Fritillaria, 46 from Cuscuta, 144 from Atractylodes, 225 from Saposhnikovia, 124 from Wolfiporia cocos, 150 from Dried tangerine peel, 401 from Licorice, and 158 from Epimedium brevicornu. Corresponding to these active ingredients, a total of 502 potential drug targets were identified, with 269 potential targets from Ginseng, 162 from Astragalus, 3 from Ophiopogon, 17 from Schisandra, 100 from Aster Tataricus, 89 from Fritillaria, 61 from Cuscuta, 33 from Atractylodes, 51 from Saposhnikovia, 27 from Wolfiporia cocos, 40 from Dried tangerine peel, 74 from Licorice, and 105 from Epimedium brevicornu. A drug-active ingredient-target interaction network for LJF was constructed using Cytoscape 3.7.2 software, resulting in a total of 2564 nodes and 3367 edges (Figure 1).

Disease Target Screening for COPD

The screening criteria were established as follows: ① "Chronic Obstructive Pulmonary Disease"; ② Species: human. Our study utilized the chip dataset GSE148004 (which includes 7 cases of COPD sputum tissue and 9 healthy control sputum tissue samples) as an internal test set, while the chip dataset GSE212331 (which includes 72 cases of COPD sputum tissue and 15 healthy control sputum tissue samples) served as the external validation set. After background correction and normalization of the data, sample distribution plots are shown in Figures 2A and 3A. Based on the criteria of P value ($P < 0.05$) and expression fold change ($|\log2FC| \geq 1.00$), a total of 1196 upregulated differentially expressed genes (DEGs) and 752 downregulated DEGs were identified in the GSE148004 dataset. In the GSE212331 dataset, 389 upregulated DEGs and 250 downregulated DEGs were obtained. Heatmaps for the DEGs after differential analysis are shown in Figures 2B and 3B. The processed data were imported into R software to create volcano plots, as seen in Figures 2C and 3C. After sorting the differentially expressed genes associated with COPD by log2FC, GSEA analysis revealed that the gene set from the GSE148004 dataset was significantly enriched in pathways such as Aminoacyl−tRNA biosynthesis, Ascorbate and aldarate metabolism, Bladder cancer, Citrate cycle (TCA cycle), Glycosaminoglycan biosynthesis − chondroitin sulfate / dermatan sulfate, and IL−17 signaling pathway (Figure 2D). The gene set from the GSE212331 dataset was significantly enriched in pathways including Citrate cycle (TCA cycle), Maturity onset diabetes of the young, Nicotine addiction, Other glycan degradation, and Pantothenate and CoA biosynthesis (Figure 3D).

Differentially Expressed Genes Related to Treg/Th17 Immune Cells in COPD

Treg/Th17 immune cell-related genes were obtained from the CellMarker website (http://xteam.xbio.top/CellMarker/#), and their expression matrix was extracted. Based on the criterion of P value ($P < 0.05$) for screening differentially expressed genes (DEGs), a total of 89 upregulated DEGs and 121 downregulated DEGs were identified in the GSE148004 dataset, while 35 upregulated DEGs and 38 downregulated DEGs were identified in the GSE212331 dataset. Heatmaps of the expression matrices were generated, as shown in Figure 4A and B.

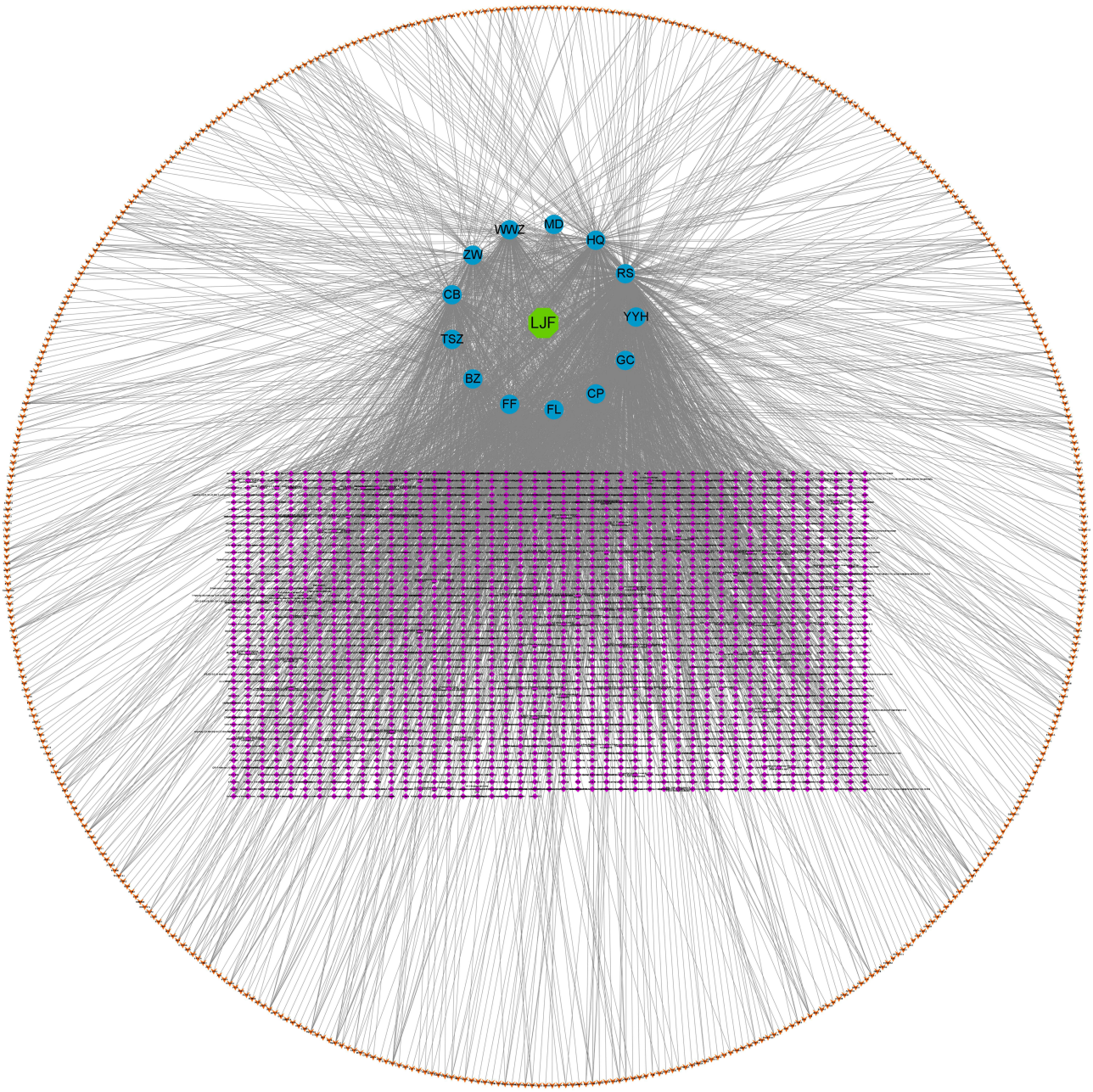

Figure 1 LJF-Active Ingredients-Target Interaction Network. The 13points represented by small circles correspond to 13 types of TCM in LJF; the 2048 nodes arranged in rectangular shapes within the network represent the active components of LJF, while the 502 nodes depicted as large circles correspond to the targets associated with these active components.

Relative Expression of Core Genes and ROC Model Construction

The previously identified 502 drug active ingredient targets were compared against 210 COPD-related genes from the GSE148004-IMM dataset and 73 COPD-related genes from the GSE212331-IMM dataset using the online Venn diagram creation tool InteractiVenn. This mapping resulted in the identification of three potential therapeutic targets for LJF in COPD: IL10, KCNN4, and BIRC3, as shown in Figure 5A. To further clarify the expression changes of these three Treg/Th17 immune cell-related genes in COPD, expression data related to COPD was downloaded from GEO using the GSE212331 dataset for validation. The relative expression levels of the three Treg/Th17 immune cell genes were analyzed using the ggpubr package, and boxplots of the expression levels were generated, as shown in Figure 5B. The results indicated that the expression of KCNN4 and other genes significantly downregulatedin COPD ($p < 0.05$), while IL10 and BIRC3 also exhibited significantly

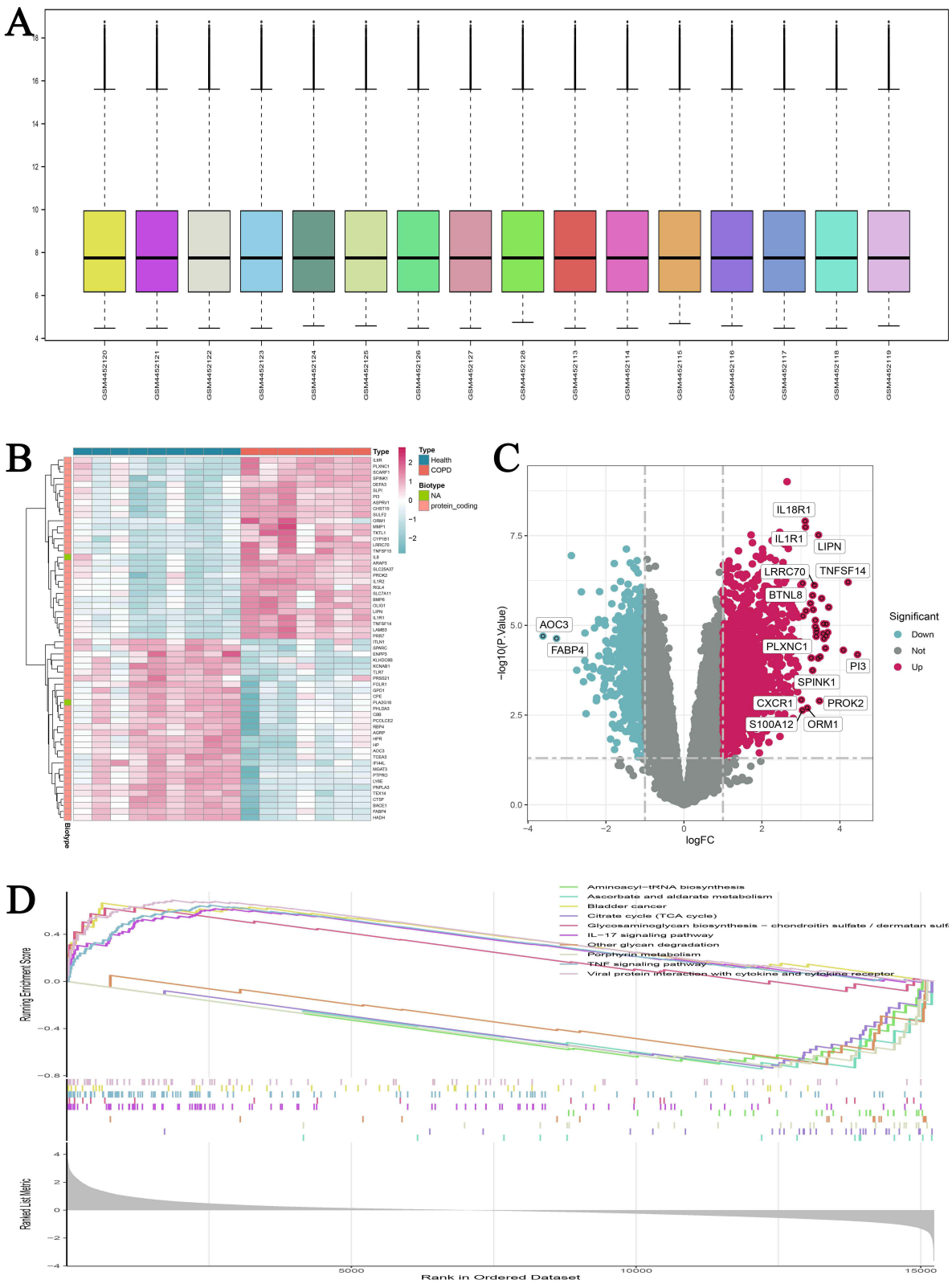

Figure 2 Target Selection for COPD (GSE148004): This includes sputum samples from 7 cases of COPD and sputum samples from 9 healthy control subjects. (**A**) Normalized sample distribution of GSE148004. (**B**) Heatmap of differentially expressed genes in GSE148004. Based on a P value < 0.05 and a fold change≥2.00 (| log2FC|≥1.00) as criteria for screening differentially expressed genes. (**C**) Volcano plot of differentially expressed genes in GSE148004; (**D**) Gene Set Enrichment Analysis (GSEA) of GSE148004.

https://doi.org/10.2147/COPD.S512469

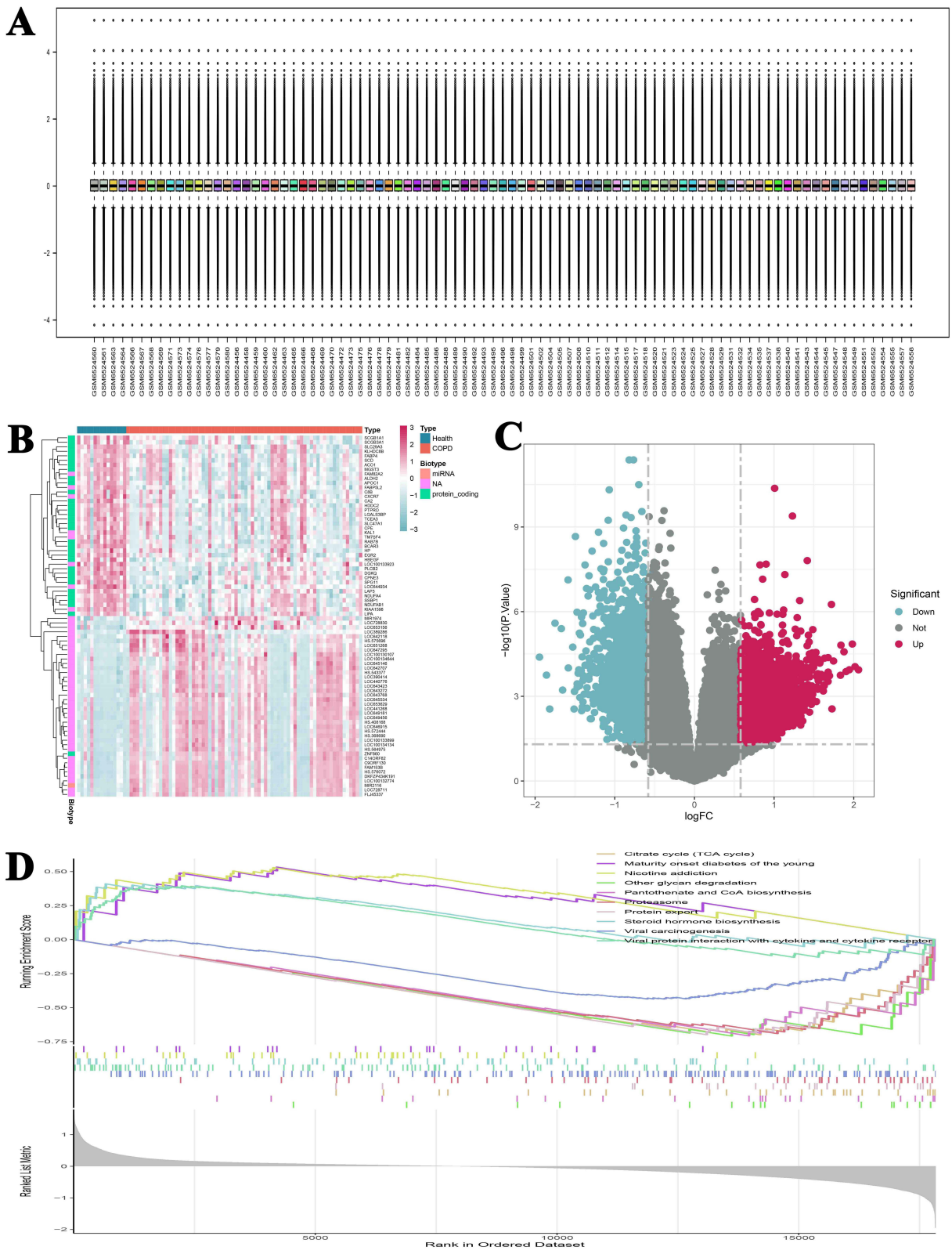

Figure 3 Target Selection for COPD (GSE212331): This includes sputum samples from 72 cases of COPD and sputum samples from 15 healthy control subjects. (**A**) Normalized sample distribution of GSE212331. (**B**) Heatmap of differentially expressed genes in GSE212331. Based on a P value < 0.05 and a fold change≥2.00 (|log2FC|≥1.00) as criteria for screening differentially expressed genes. (**C**) Volcano plot of differentially expressed genes in GSE212331; (**D**) Gene Set Enrichment Analysis (GSEA) of GSE212331.

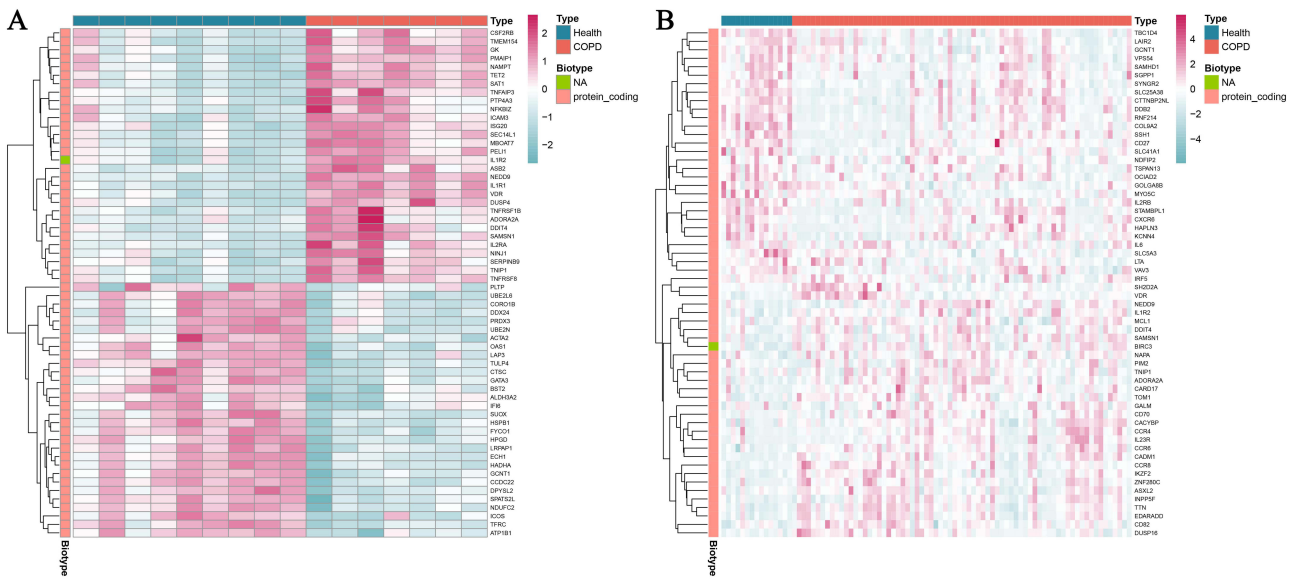

Figure 4 Target Selection for COPD Treg/Th17 Immune Cells. (Relevant genes associated with Treg/Th17 immune cells were obtained from the CellMarker website, and their expression matrix was extracted. Differentially expressed genes were identified based on a P value < 0.05 as the screening criterion.) (**A**). Heatmap of GSE148004-IMM. (**B**) Heatmap of GSE212331-IMM.

upregulation expression in COPD ($p < 0.05$). ROC curve analysis was performed on the above genes to evaluate their sensitivity and specificity for diagnosing COPD, as depicted in Figure 5C. The results indicated that for the GSE212331 dataset, the area under the curve (AUC) for IL10, KCNN4, and BIRC3 genes was greater than 0.65, demonstrating good diagnostic significance.

Immune Infiltration Analysis of Core Targets in COPD

The expression matrix data GSE212331 for COPD was analyzed using the CIBERSORT package to estimate the immune cell composition. Furthermore, CIBERSORT was utilized to analyze the composition of immune cells in each sample and generate bar plots, as shown in Figure 6A. Finally, the corrplot package was employed to analyze the interactions among immune cell populations in COPD, and a co-expression map of immune cell infiltration in COPD was generated, as shown in Figure 6B. The results indicated that the quantity of regulatory T cells (Tregs) was significantly decreased in COPD ($p < 0.05$).

GO and KEGG Enrichment Analysis Results

GO and KEGG pathway enrichment analyses were conducted on the potential targets related to Treg/Th17 immune cells in COPD using the Bioconductor and clusterProfiler packages in R. The results showed that the GO analysis of potential target genes primarily enriched for biological processes related to positive regulation of protein secretion, positive regulation of peptide secretion, and positive regulation of secretion by cells. For cellular components, the enrichment included voltage-gated potassium channel complex, potassium channel complex, and cation channel complex. The molecular functions were mainly enriched in calcium-activated potassium channel activity, calcium-activated cation channel activity, and cysteine-type endopeptidase inhibitor activity involved in apoptotic processes, as shown in Figure 7A and B. The KEGG pathway enrichment analysis revealed that the primary pathways were concentrated on Toxoplasmosis, Asthma, and Apoptosis, as depicted in Figure 7C and D.

Screening of LJF Components

Molecular docking studies were conducted on the screened components of LJF to identify potential candidate drugs targeting the core targets IL10 and BIRC3. The PDB structures of the core proteins IL10 and BIRC3 were downloaded. Ultimately, a total of 211 TCM components met the screening criteria. All these compounds were docked with the core proteins IL10 and BIRC3 and ranked based on their LibDock scores. It was found that BIRC3 formed stable docking

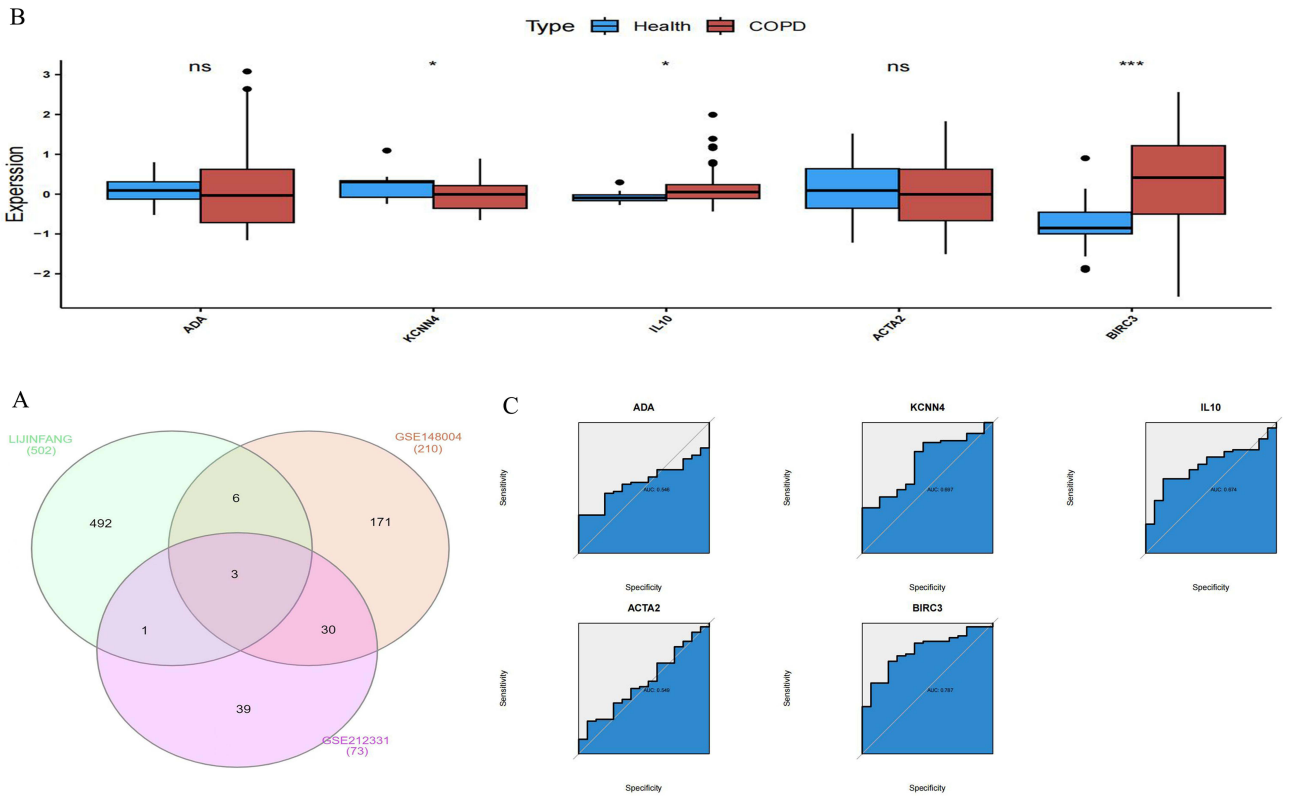

Figure 5 Relative Expression Levels of Core Genes and ROC Model Construction. (**A**) Venn diagram of intersections. The 502 drug active component targets were matched and mapped with 210 COPD-related genes from GSE148004-IMM and 73 COPD-related genes from GSE212331-IMM, resulting in the identification of three potential therapeutic targets of LJF for COPD: IL10, KCNN4, and BIRC3. (**B**) Relative Expression Levels of Core Genes in GSE212331. (**C**) ROC Model of Core Differentially Expressed Genes in GSE212331 Samples. (*p<0.05, ***p<0.001).

models with the TCM components MOL004903 (Liquiritin), MOL004860 (Licorice glycoside E), and MOL000433 (FA), while IL10 interacted stably with MOL004860 (Licorice glycoside E), MOL004917 (Glycyroside), and MOL004492 (Chrysanthemaxanthin), indicating potential targeting of IL10 and BIRC3, as shown in Figure 8. We further employed AutoDock-Vina for more accurate docking related to essential components of the core proteins. The selected candidate drugs targeting the active sites of IL10 and BIRC3 included MOL004903 (Liquiritin), MOL004860 (Licorice glycoside E), MOL000433 (FA), MOL004917 (Glycyroside), and MOL004492 (Chrysanthemaxanthin), all exhibiting affinities of −5.5 kcal·mol^{-1}or lower. Considering RMSD, chemical energy, and docking scores, MOL004860 (Licorice glycoside E) showed the most stable docking conformation with the Treg/Th17 immune cell target IL10, followed by MOL004860 (Licorice glycoside E) with BIRC3. This suggests they may provide promising drugs for Treg/Th17 immune cells in patients with COPD, as detailed in Table 1 and Figure 9. Overall, the analysis indicates that MOL004860 (Licorice glycoside E) may prevent or treat COPD by targeting and regulating the expression of the Treg/Th17 immune cell target IL10.

Results of Flow Cytometry Detection with Optimal Concentration of CSE

Treatment of rat PBMCs with 1% CSE resulted in an initial upregulation of Treg and Th17 cells. However, treatment with 5% CSE caused a marked downregulation of Treg cells, while the upregulation of Th17 cells was more pronounced. Furthermore, concentrations of 10% and 30% CSE led to a further decrease in Treg cells and an increase in Th17 cells (Figure 10).

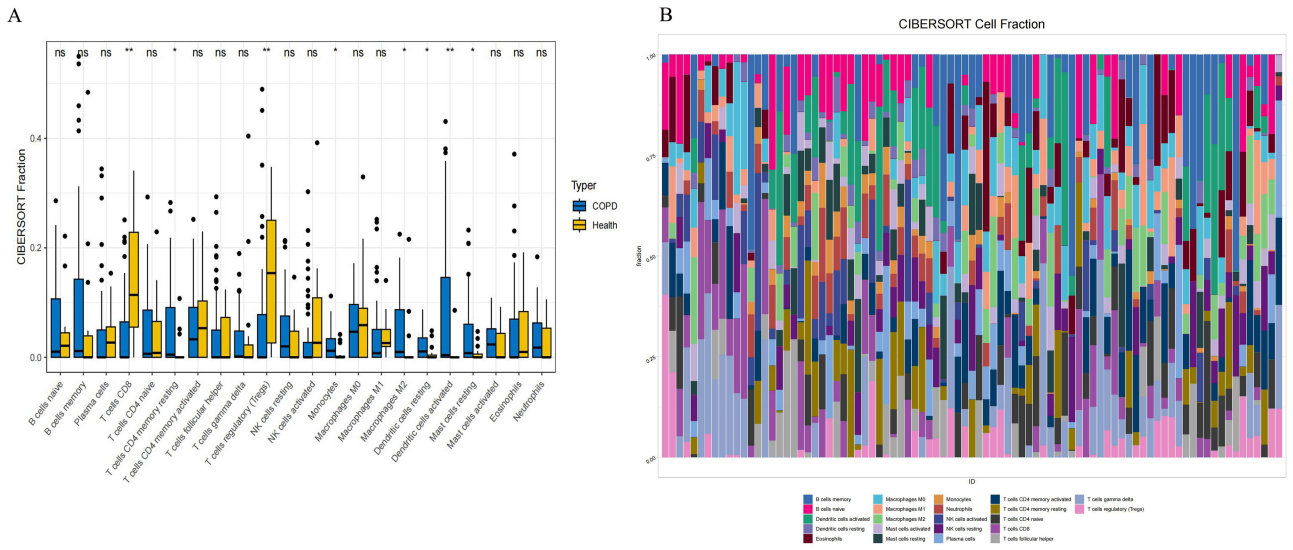

Figure 6 Immune Cell Infiltration Analysis. (**A**) Bar Chart of Immune Cell Distribution. (**B**) Heatmap of Immune Cell Interactions. (*p<0.05, **p<0.01).

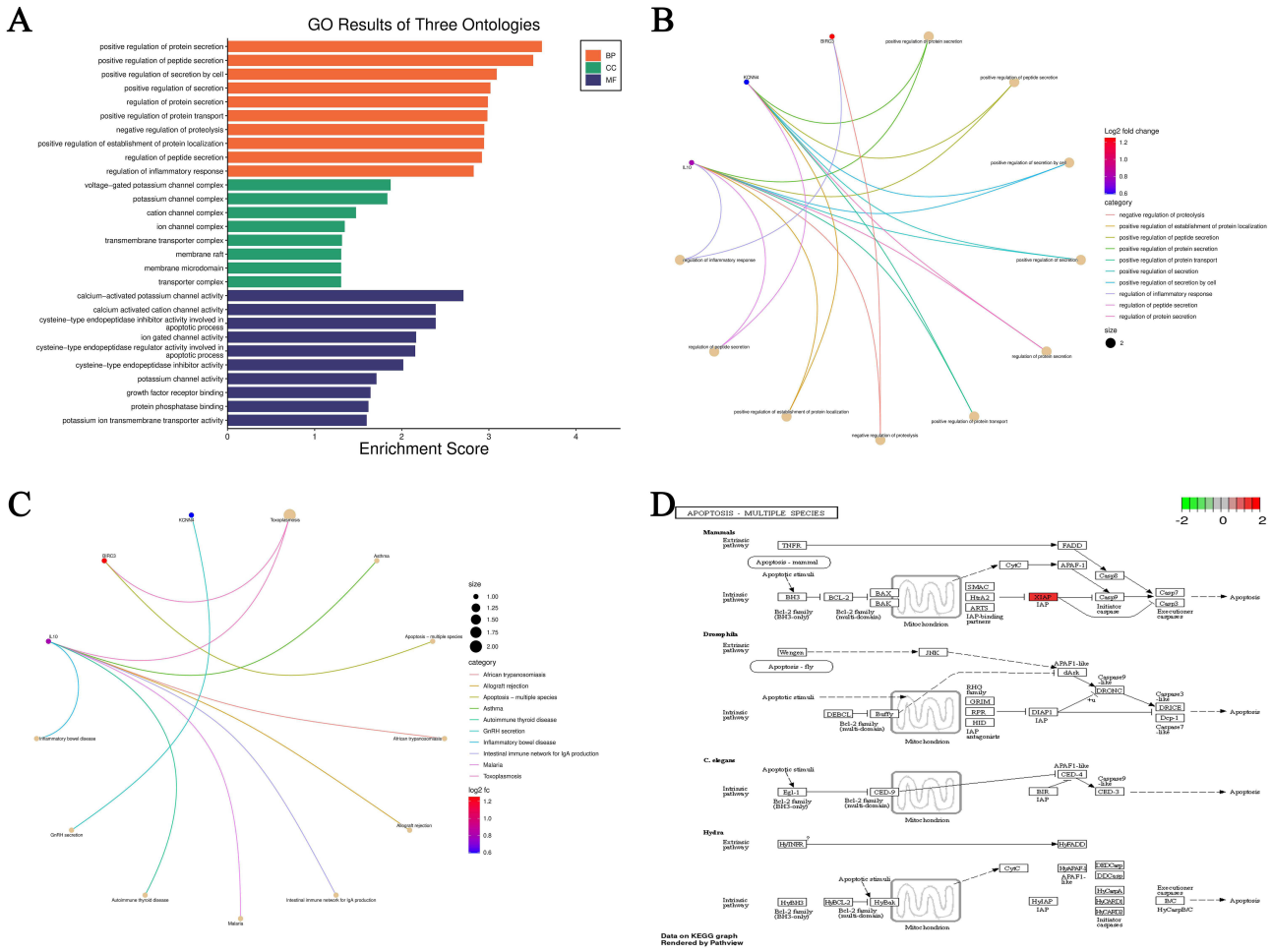

Figure 7 Enrichment Analysis (IL10, KCNN4, and BIRC3). (**A**) Bar Chart of GO Functional Analysis; (**B**) Chord Diagram of GO Enrichment Analysis; (**C**) Chord Diagram of KEGG Analysis; (**D**) Apoptosis Signaling Pathway.

https://doi.org/10.2147/COPD.S512469

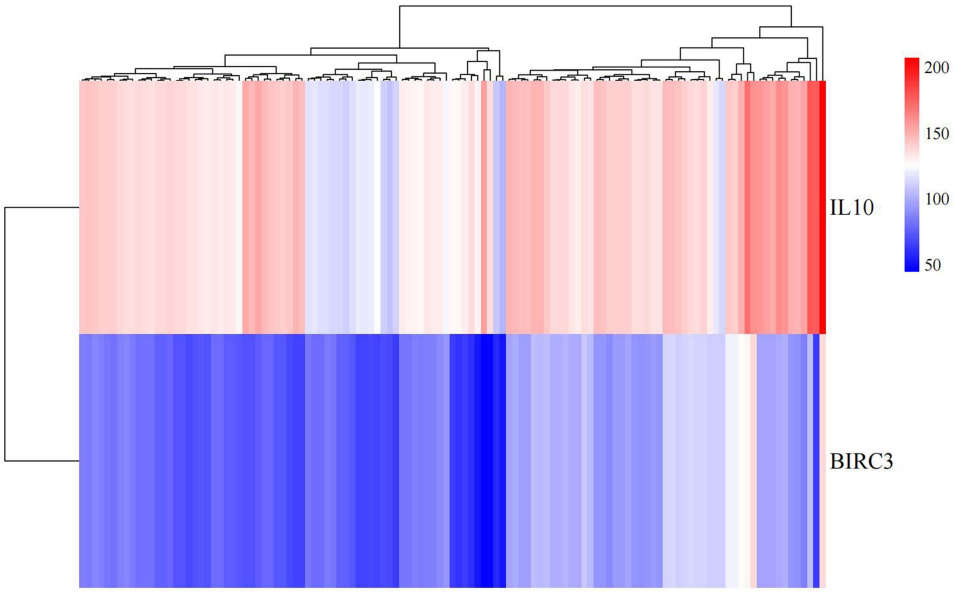

Figure 8 Molecular Docking Simulation.

Results of Flow Cytometry, ELISA, and Western Blotting Analyses

Compared to the Control group, flow cytometry analysis in the CSE group showed a downregulation of Treg and an upregulation of Th17 cells (Figure 11). ELISA results indicated that the expression levels of IL-17, TNF-α, IL-1-β, and IL-10 were upregulated (Figure 12A). In the CSE+LJF-L and CSE+LJF-H groups compared to the CSE group, flow cytometry results revealed a significant upregulation of Treg cells and a significant downregulation of Th17 cells (Figure 11). ELISA analysis showed that the expression levels of pro-inflammatory cytokines IL-17, TNF-α, and IL-1β were significantly downregulated, while the expression level of the anti-inflammatory cytokine IL-10 was markedly upregulated (Figure 12A). Western Blotting analysis demonstrated that the expression of KCNN4 protein was down-regulated in the CSE group compared to the Control group, while the expression of IL-10 and BIRC3 proteins was upregulated (Figure 12B). In the CSE+LJF-L and CSE+LJF-H groups compared to the CSE group, KCNN4 protein expression was upregulated, with IL-10 protein expression showing a more pronounced increase, while BIRC3 protein expression was downregulated (Figure 12B).

Table 1 Molecular Docking Results from Autodock Vina and Discovery Studio 2019

Protein (Binding Site)	Compound	Vina (kcal mol^{-1})	[1]RMSD	[2]DS
[3]BIRC3(6W74)	MOL004903 (liquiritin)	−6.6	0.921	138.907
BIRC3(6W74)	MOL004860 (licorice glycoside E)	−7.1	1.944	137.537
BIRC3(6W74)	MOL000433 (FA)	−6.2	1.918	128.553
[4]IL10(IL10)	MOL004860 (licorice glycoside E)	−6.4	1.507	207.182
IL10(IL10)	MOL004917 (glycyroside)	−6.0	1.869	179.067
IL10(IL10)	MOL004492 (Chrysanthemaxanthin)	−5.5	1.811	176.859

Notes: 1.Root - Mean - Square Deviation, 2.LibDockScore, 3.Baculoviral IAP repeat-containing protein 3, 4. Interleukin-10.

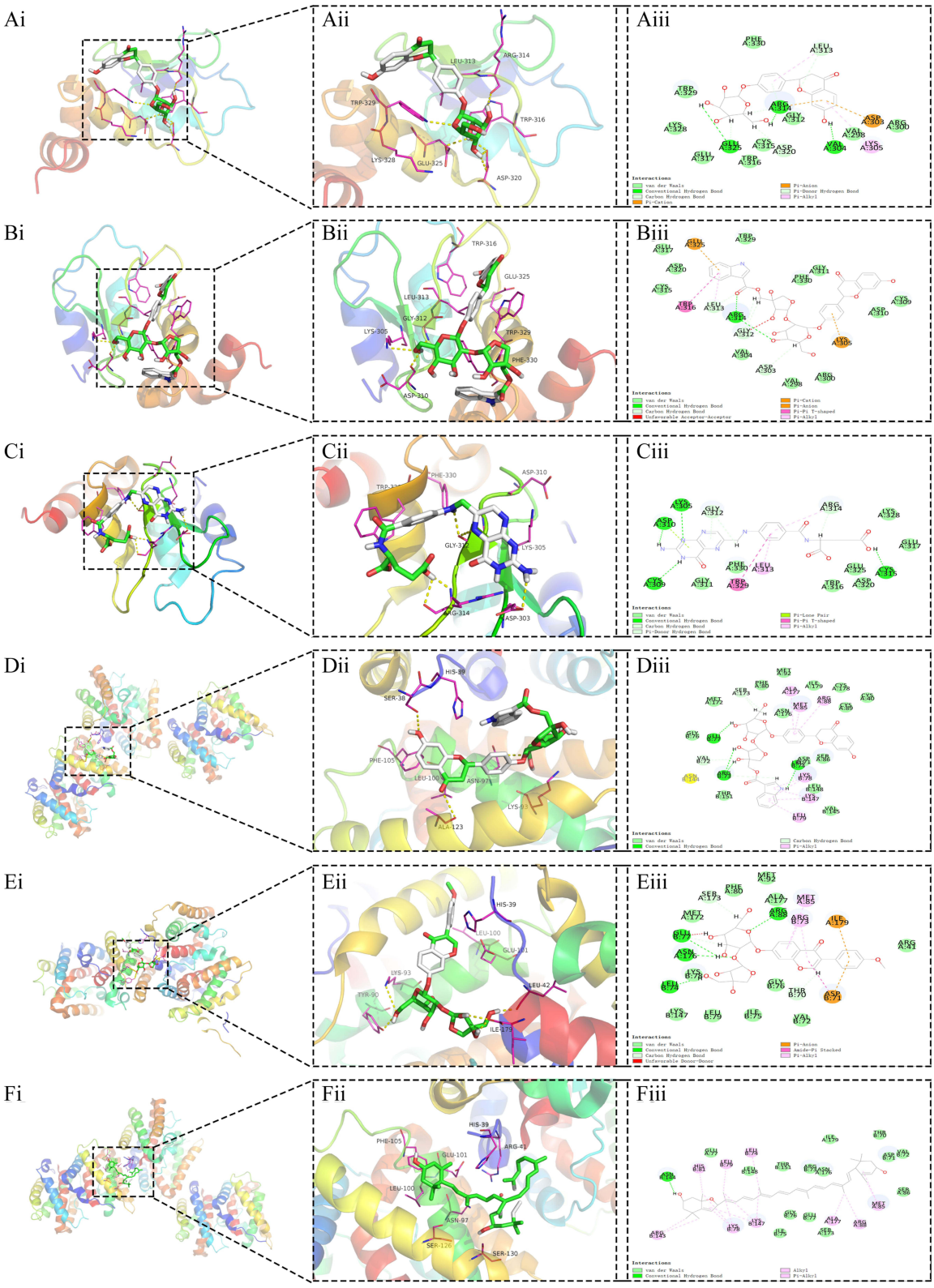

Figure 9 Molecular Docking Model. (**A**i) BIRC3-MOL004903-3D (macroscopic). (**A**ii) BIRC3-MOL004903-3D (microscopic). (**A**iii) BIRC3-MOL004903-2D. (**B**i) BIRC3-MOL004860-3D (macroscopic). (**B**ii).BIRC3-MOL004860-3D (microscopic). (**B**iii) BIRC3-MOL004860-2D. (**C**i) BIRC3-MOL000433-3D (macroscopic). (**C**ii) BIRC3-MOL000433-3D (microscopic). (**C**iii) BIRC3-MOL000433-2D. (**D**i). IL10-MOL004860-3D (macroscopic).(**D**ii). IL10-MOL004860-3D (microscopic). (**D**iii). IL10-MOL004860-2D.(**E**i). IL10-MOL004917-3D (macroscopic). (**E**ii) IL10-MOL004917-3D (microscopic). (**E**iii) IL10-MOL004917-2D. (**F**i) IL10-MOL004492-3D (macroscopic). (**F**ii) IL10-MOL004492-3D (microscopic). (**F**iii) IL10-MOL004492-2D.

https://doi.org/10.2147/COPD.S512469

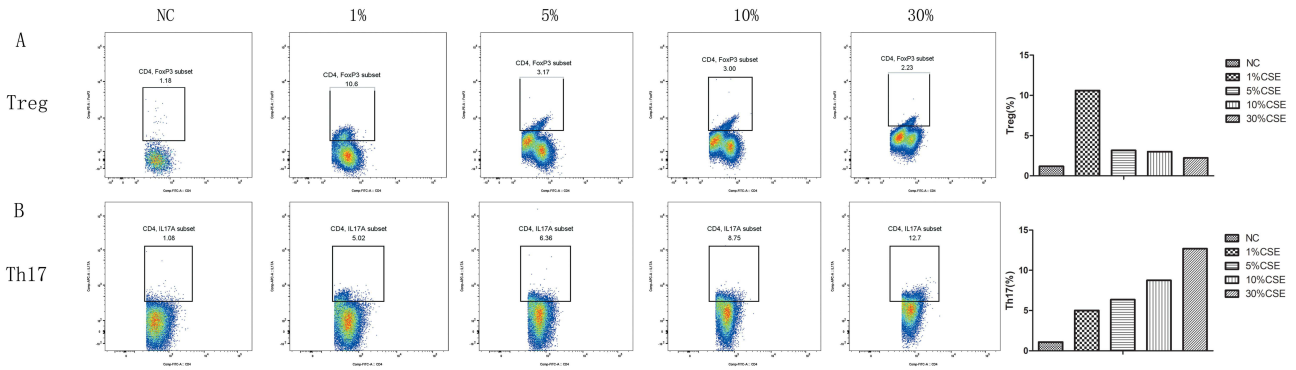

Figure 10 Flow Cytometry Results of Optimal CSE Treatment Concentration. CSE treatment leads to a decrease in Treg cells and an upregulation of Th17 cells. (**A**) Percentage of Treg cells after intervention with different concentrations of CSE in PBMCs. (**B**) Percentage of Th17 cells after intervention with different concentrations of CSE in PBMCs.

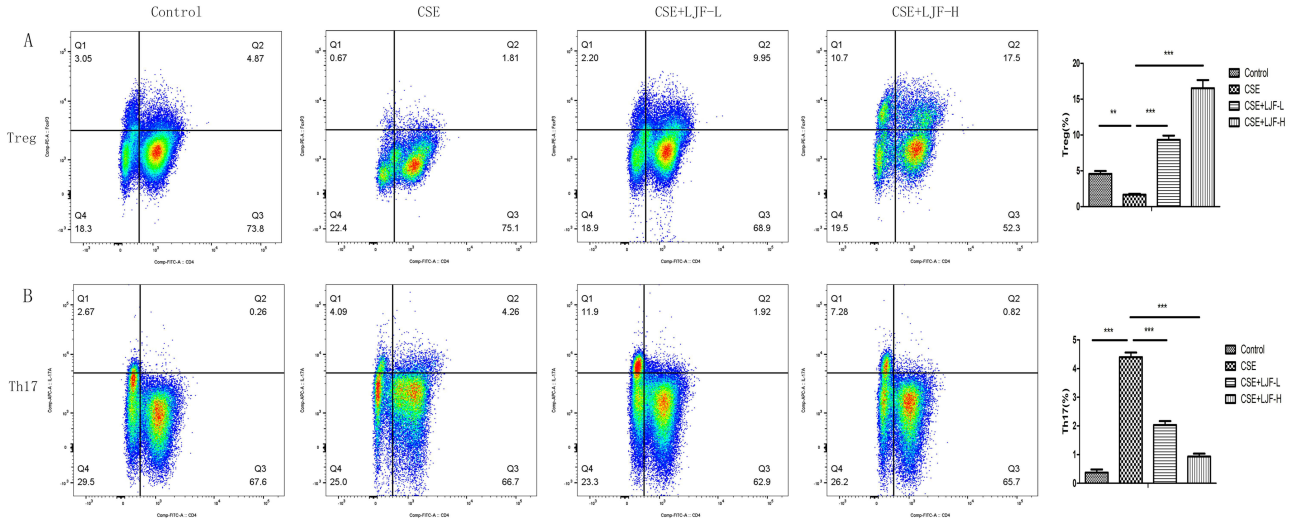

Figure 11 Flow Cytometry Results for Treg (CD3+CD4+FOXP3+) / Th17 (CD3+CD4+IL17) Detection. LJF can reverse the decrease in Treg cells and the upregulation of Th17 cells induced by CSE. (**A**). Percentage of Treg cells in the Control group, CSE group, CSE+LJF-L group, and CSE+LJF-H group. (**B**). Percentage of Th17 cells in the Control group, CSE group, CSE+LJF-L group, and CSE+LJF-H group. (N=3. ***p<0.001, **p<0.01.).

Discussion

The imbalance between Treg and Th17 cells is critical in COPD pathogenesis. Th17 cells secrete IL-17, which binds to IL-17R, playing a key role in defense against extracellular bacterial infections, mediating chronic inflammation, and contributing to autoimmune diseases.[18] Treg cells secrete anti-inflammatory cytokines such as IL-10 and TGF-β, which inhibit the activation and proliferation of Th17 cells, thereby maintaining immune homeostasis. Additionally, Treg cells decrease levels of IL-17 and INF-γ, suppressing inflammatory responses.[18,19] In COPD patients, the proportion of Th17 cells is increased.[20]

TCM has been demonstrated to have a clear therapeutic effect on COPD.[5] In our preliminary studies, LJF showed experimental therapeutic effects in animal models.[21] LJF is an approved herbal prescription used at the Department of Respiratory and Critical Care Medicine of the Affiliated Ruikang Hospital, Guangxi University of Chinese Medicine. The version of LJF used in this study is a modified formula, which removes gecko and adds Cuscuta and Epimedium brevicornu, while ginseng is substituted for Dangshen. The integration of multiple drugs, various components, and extensive targets in traditional Chinese herbal formulas has hindered the investigation of their potential mechanisms of action in the treatment of COPD.[5,22] In this study, we systematically confirmed the therapeutic effects of LJF on COPD through network pharmacology, molecular docking, and in vitro cell experiments, while exploring its potential molecular

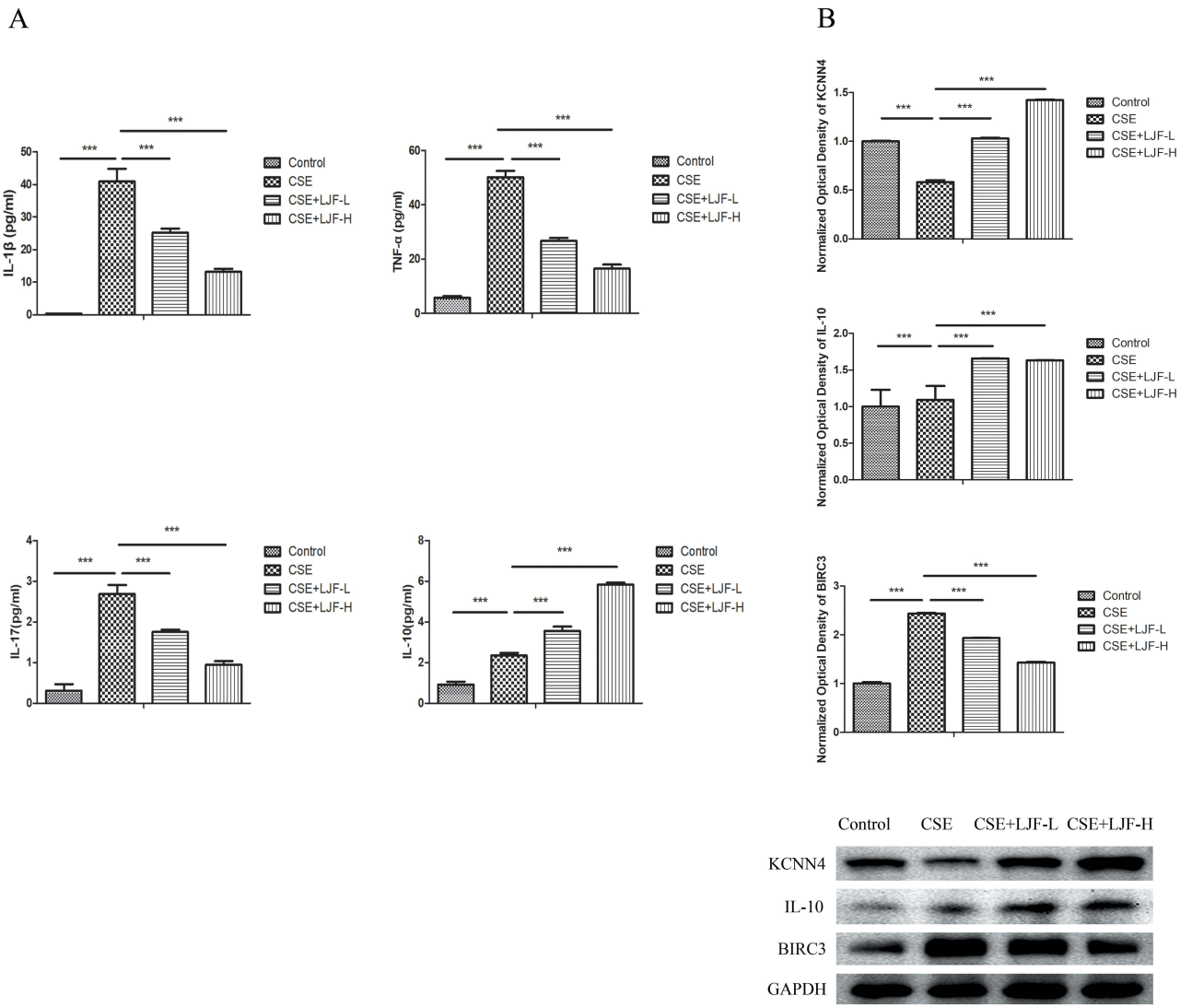

Figure 12 ELISA Detection of Expression Changes in IL-17, IL-10, TNF-α, and IL-1β in Cell Supernatant; WB Detection Results of KCNN4, IL-10, and BIRC3 Protein Expression. LJF can reverse the upregulation of IL-17, TNF-α, and IL-1β induced by CSE and enhance the upregulation of IL-10 expression. LJF can also reverse the downregulation of KCNN4 and the upregulation of BIRC3 protein expression. induced by CSE and further enhance the upregulation of IL-10 protein expression. (**A**) Expression of relevant cytokines in the Control group, CSE group, CSE+LJF-L group, and CSE+LJF-H group. (**B**) Expression of relevant proteins in the Control group, CSE group, CSE+LJF-L group, and CSE+LJF-H group. (N=3. ***p<0.001).

mechanisms. Our findings suggest that LJF can restore the balance between Treg and Th17 cells, thereby exerting anti-inflammatory effects and improving COPD.

First, we conducted a retrieval through the SymMap, TCMID, TCMSP, and TCM-ID databases, identifying 2048 active components in LJF while also obtaining 502 corresponding targets. The interaction network constructed using Cytoscape 3.7.2 includes 2564 nodes and 3367 edges, reflecting the complex relationships between components and targets. Different components may have distinct pharmacological effects, and their complementary interactions can enhance overall therapeutic efficacy. For instance, ginseng has a significant role in modulating immune functions, while astragalus exhibits good anti-inflammatory properties.[23,24]

In the GEO database, we identified 1,196 upregulated and 752 downregulated differentially expressed genes in the GSE148004 dataset, as well as 389 upregulated and 250 downregulated genes in the GSE212331 dataset. GSEA analysis indicated significant enrichment of the COPD differential gene set in GSE148004 in pathways such as aminoacyl−tRNA biosynthesis, ascorbate and aldarate metabolism, bladder cancer, citrate cycle (TCA cycle), glycosaminoglycan biosynthesis (chondroitin sulfate/dermatan sulfate), and the IL−17 signaling pathway. Similarly, the differential gene set in

 https://doi.org/10.2147/COPD.S512469

GSE212331 showed enrichment in pathways including the citrate cycle, maturity onset diabetes of the young, nicotine addiction, other glycan degradation, and pantothenate and CoA biosynthesis. We obtained Treg/Th17 immune cell-related genes from the CellMarker website, identifying 210 COPD-GSE148004-IMM related genes and 73 COPD-GSE212331-IMM related genes. Venn diagram matching with the previously identified 502 active component targets of LJF revealed three potential therapeutic targets for LJF in COPD: IL10, KCNN4, and BIRC3.

Validation with the GSE212331 dataset revealed a significant decrease in KCNN4 gene expression in COPD, alongside a notable upregulation of IL-10 and BIRC3. ROC curve analysis showed that the AUC values for IL-10, KCNN4, and BIRC3 exceeded 0.65, indicating strong diagnostic potential for COPD.

Our results suggest that LJF may influence the Treg/Th17 cell balance in COPD by modulating the expression of IL-10, KCNN4, and BIRC3. Previous studies indicate that IL-10 has an anti-inflammatory role in the inflammatory response, with low IL-10 expression levels associated with increased COPD severity.[25] Moreover, a prospective study focusing on patients with COPD complicated by pulmonary hypertension (COPD-PH) likewise demonstrated a negative correlation between IL-10 levels and the severity of COPD-PH.[26] As a calcium-dependent potassium channel, KCNN4 has been shown to influence mucus adhesion, neutrophil infiltration, and emphysema in obstructive lung diseases, and it can also activate the NLRP3 inflammasome.[27,28] Interleukin-1 beta (IL-1β) and TNF-α can induce an increase in BIRC3 mRNA expression, indicating that BIRC3 is upregulated in response to inflammatory cytokine stimulation.[29] BIRC3 is significantly elevated in induced sputum from patients with asthma and shows a positive correlation with airway eosinophilia, peripheral blood allergic inflammatory markers, type 2 cytokines, and airway obstruction.[30] This suggests that BIRC3 may be involved in the pathogenesis of asthma by influencing eosinophils and allergic inflammation.

The Treg/Th17 cell balance has recently emerged as a novel approach in immunotherapy for COPD.[18,31] Despite numerous studies on therapeutic strategies targeting the Treg/Th17 cell balance, effective medications for COPD treatment remain lacking in clinical practice.[32] Furthermore, screening active components from TCM formulations with demonstrated clinical efficacy presents a viable strategy for new drug development.

We found a decrease in the quantity of Tregs immune cells in COPD through immune infiltration analysis. GO/KEGG enrichment analysis revealed that IL-10, KCNN4, and BIRC3 were mainly concentrated in pathways related to Toxoplasmosis, Asthma, and Apoptosis. Subsequently, we conducted molecular docking of the active components of LJF to identify potential candidate drugs that target the core targets IL10 and BIRC3. Molecular docking is a tool for analyzing receptor-ligand interactions through electrostatic forces and predicting their binding modes.[33] It is a crucial method in drug discovery and development, with widespread application in the modernization of TCM in recent years.[34] Our results indicate that the docking model formed by MOL004860 and the Treg/Th17 immune cell target IL10 is the most stable The monomer MOL004860 may aid in the prevention and treatment of COPD by targeting and regulating IL10 expression, providing a promising drug for modulating the Treg/Th17 balance in COPD patients.

Next, we used CSE to stimulate rat PBMCs in vitro to verify that CSE can disrupt immune balance, leading to the development of inflammatory diseases. Our results indicate that 1% CSE may sufficiently activate the immune system, resulting in an initial upregulation of Treg and Th17 cells, indicative of an acute phase immune response. Conversely, 5% CSE can cause a significant downregulation of Treg cells, suggesting a weakened anti-inflammatory response, while the upregulation of Th17 cells may enhance inflammatory responses, consistent with findings from previous animal studies.[35]

Our results show that IL-17, TNF-α, IL-1β, and IL-10 levels are upregulated in the CSE intervention group. Treatment with low-dose or high-dose LJF significantly increases the proportion of Treg cells and decreases Th17 cells. Concurrently, pro-inflammatory cytokines IL-17, TNF-α, and IL-1β are downregulated, while the anti-inflammatory cytokine IL-10 is upregulated. These findings suggest that LJF treatment effectively restores the balance between Treg and Th17 cells in the CSE-treated cellular model and modulates inflammatory cytokine expression. Similar to other reported TCM formulations,[35] LJF demonstrated potential anti-inflammatory and immunoregulatory effects.

Bioinformatics analysis indicates a significant downregulation of genes like KCNN4 in COPD, while IL-10 and BIRC3 are significantly upregulated. Our WB results show that CSE treatment downregulates KCNN4 and upregulates BIRC3 expression. Furthermore, LJF treatment can reverse these changes. These findings suggest that LJF may exert therapeutic effects on COPD by modulating the expression of KCNN4 and BIRC3.

Previous research has demonstrated that the knockout of the KCNN4 gene enhances ciliary beating frequency and mucociliary clearance in the airways.[27] However, this study primarily focused on epithelial cells, and the expression of KCNN4 in PBMCs under CSE induction has not been reported. Our study is the first to report the downregulated of KCNN4 expression in PBMCs induced by CSE, and that LJF can reverse this downregulated. Inflammatory factors can induce the upregulation of BIRC3 expression,[29,30] which is consistent with the results observed in our study where CSE induced inflammation in PBMCs. Additionally, LJF can also reverse the upregulation of BIRC3 expression.

Many studies have confirmed that IL-10 is a major anti-inflammatory cytokine that is significantly downregulated in patients with COPD.[26,36] Interestingly, our study found that the WB results for IL-10 were consistent with the ELISA findings, showing an upregulation after CSE treatment that was further enhanced by LJF treatment. In inflammatory diseases like COPD, this upregulation may reflect a natural cellular response to secrete IL-10 to mitigate inflammatory damage, with LJF potentially promoting IL-10 secretion.

Future research should include animal experiments and clinical trials to validate the therapeutic effects and mechanisms of LJF in COPD. It is also essential to assess the long-term safety and efficacy of LJF in diverse COPD populations. Additionally, further investigation can explore the specific roles of KCNN4 and BIRC3 in COPD pathology, particularly within immune cell subsets.

Conclusion

In summary, our study demonstrates that LJF can effectively restore the balance between Treg and Th17 cells and exert anti-inflammatory effects by constructing a CSE-induced PBMC cellular model. Although the biological mechanisms underlying LJF's treatment of COPD are highly complex, involving multiple targets and pathways, we have further investigated its mechanisms. The monomer MOL004860 may potentially regulate the expression of the Treg/Th17 immune cell target IL-10 to prevent and treat COPD. Ultimately, we identified three key targets for further focused investigation, demonstrating that LJF may exert its anti-inflammatory and immunoregulatory effects by modulating KCNN4, BIRC3, and IL-10. Our findings identify potential targets through which LJF regulates the Treg/Th17 balance in COPD, offering new insights into the use of TCM for its treatment. Future research will include animal experiments to further validate the long-term safety and efficacy of LJF in COPD. Additionally, subsequent studies should focus on targeted drug design and the development of improved formulations of LJF.

Animal Ethics Statement

The animal use protocol has been reviewed and approved by the Guangxi University of Chinese Medicine Institutional Animal Welfare and Ethical Committee.The guiding principles for laboratory animal welfare are the internationally recognized "3Rs" principles (Replacement, Reduction, and Refinement).All animal husbandry and experimentation were conducted in strict accordance with the regulations governing the management and use of laboratory animals.

Declaration of Generative AI and AI-Assisted Technologies in the Writing Process

Statement: During the preparation of this work the author(s) used Librechat (https://www.librechat.cloud/) in order to Academic writing. After using this tool/service, the author(s) reviewed and edited the content as needed and take(s) full responsibility for the content of the published article.

Author Contributions

All authors made a significant contribution to the work reported, whether that is in the conception, study design, execution, acquisition of data, analysis and interpretation, or in all these areas; took part in drafting, revising or critically reviewing the article; gave final approval of the version to be published; have agreed on the journal to which the article has been submitted; and agree to be accountable for all aspects of the work.

Funding

This work was supported by the National Natural Science Foundation of China (Project No. 82360908),the Guangxi Traditional Chinese Medicine Key Research Laboratory Construction Project-the Guangxi Traditional Chinese Medicine Chronic Lung Disease Prevention and Treatment Key Laboratory (Document No. Guangxi CM science and education development [2023] Number 9), the third batch of the "Qihuang Project" high-level talent team cultivation initiative at Guangxi University of Traditional Chinese Medicine-the Integrated Chinese and Western Medicine Innovation Team for Lung Disease Prevention and Treatment (Project No. 202412).

Disclosure

The authors declare that there are no competing interests associated with this paper.

References

1. Wu Y, Shen P, Yang Z, et al. Association of walkability and fine particulate matter with chronic obstructive pulmonary disease: a cohort study in China. *Sci Total Enviro*. 2023;858:159780. doi:10.1016/j.scitotenv.2022.159780
2. Patel N. An update on COPD prevention, diagnosis, and management: the 2024 GOLD report. *Nur Practitioner*. 2024;49(6):29–36. doi:10.1097/01.NPR.0000000000000180
3. Wang C, Xu J, Yang L, et al. Prevalence and risk factors of chronic obstructive pulmonary disease in China (the China Pulmonary Health [CPH] study): a national cross-sectional study. *Lancet*. 2018;391(10131):1706–1717. doi:10.1016/S0140-6736(18)30841-9
4. Chen S, Kuhn M, Prettner K, et al. The global economic burden of chronic obstructive pulmonary disease for 204 countries and territories in 2020 - 50: a health - augmented macroeconomic modelling study. Lancet Glob Health. 2023;11(8):e1183 -
5. Cao X, Wang Y, Chen Y, et al. Advances in traditional Chinese medicine for the treatment of chronic obstructive pulmonary disease. *J Ethnopharmacol*. 2023;307:116229. doi:10.1016/j.jep.2023.116229
6. Zhanhua L, Sining C, Ruixiang L, et al. Liking prescription reduces cigarette smoke extract-induced inflammatory response via inhibiting JAK2/STAT3/ROR-γt pathway to reduce Th17/CD4+ T cell ratio in rats. *Chin J Cell Mol Immunol*. 2021;37(4):295–301.
7. Wang C, Wang H, Dai L, et al. T-helper 17 cell/regulatory T-cell imbalance in COPD combined with T2DM patients. *Int J Chronic Obstr*. 2021;16:1425–1435. doi:10.2147/COPD.S306406
8. Hopkins AL. Network pharmacology. *Nat Biotechnol*. 2007;25(10):1110–1111. doi:10.1038/nbt1007-1110
9. Lai X, Wang X, Hu Y, et al. Network pharmacology and traditional medicine. *Front Pharmacol*. 2020;11:1194. doi:10.3389/fphar.2020.01194
10. Wu Y, Zhang F, Yang K, et al. SymMap: an integrative database of traditional Chinese medicine enhanced by symptom mapping. *Nucleic Acids Res*. 2019;47(D1):D1110–D17. doi:10.1093/nar/gky1021
11. Wang Y, Liu M, Jafari M, Tang J. A critical assessment of Traditional Chinese Medicine databases as a source for drug discovery. *Front Pharmacol*. 2024;15:1303693. doi:10.3389/fphar.2024.1303693
12. Chen B, Khodadoust MS, Liu CL, Newman AM, Alizadeh AA. Profiling tumor infiltrating immune cells with CIBERSORT. *Cancer Syst Biol*. 2018:243–259.
13. Chen L, Zhang Y, Wang S, Zhang Y, Huang T, Cai Y and Liu B. (2017). Prediction and analysis of essential genes using the enrichments of gene ontology and KEGG pathways. PLoS ONE, 12(9), e0184129. doi:10.1371/journal.pone.0184129
14. Stanzione F, Giangreco I, Cole JC. Use of molecular docking computational tools in drug discovery. *Progress Med Chem*. 2021;60:273–343.
15. Li M, Zhong X, He Z, et al. Effect of erythromycin on cigarette-induced histone deacetylase protein expression and nuclear factor-κB activity in human macrophages in vitro. *Int Immunopharmacol*. 2012;12(4):643–650. doi:10.1016/j.intimp.2011.12.022
16. Jiang Y-R, Miao Y, Yang L, et al. Effect of Chinese herbal drug-containing serum for activating-blood and dispelling-toxin on ox-LDL-induced inflammatory factors' expression in endothelial cells. *Chin J Integr Med*. 2012;18:30–33. doi:10.1007/s11655-011-0849-1
17. Tian R, Liu X, Xiao Y, et al. Huang-Lian-Jie-Du decoction drug-containing serum inhibits IL-1β secretion from D-glucose and PA induced BV2 cells via autophagy/NLRP3 signaling. *J Ethnopharmacol*. 2024;323:117686. doi:10.1016/j.jep.2023.117686
18. Thomas R, Qiao S, Yang X. Th17/Treg imbalance: implications in lung inflammatory diseases. *Int J Mol Sci*. 2023;24(5):4865. doi:10.3390/ijms24054865
19. Zi C, He L, Yao H, Ren Y, He T, Gao Y. Changes of Th17 cells, regulatory T cells, Treg/Th17, IL-17 and IL-10 in patients with type 2 diabetes mellitus: a systematic review and meta-analysis. *Endocrine*. 2022;76(2):263–272. doi:10.1007/s12020-022-03043-6
20. Xiong X-F, Zhu M, Wu H-X, Fan -L-L, Cheng D-Y. Immunophenotype in acute exacerbation of chronic obstructive pulmonary disease: a cross-sectional study. *Respir Res*. 2022;23(1):137. doi:10.1186/s12931-022-02058-x
21. Sining C, Ruixiang L, Zhanhua L, Wenfeng H, Yuqing F, Haozhou W. Effect of Lijin recipe on JAK2-STAT3-RORYT signaling pathway in chronic obstructive pulmonary disease rat model. *Chin J Integrated Trad Western Med*. 2022;42(1):89–95.
22. Yang Y, Jin X, Jiao X, et al. Advances in pharmacological actions and mechanisms of flavonoids from traditional Chinese medicine in treating chronic obstructive pulmonary disease. *Evidence Based Complement Alternative Med*. 2020;2020(1):8871105. doi:10.1155/2020/8871105
23. Ratan ZA, Youn SH, Kwak Y-S, et al. Adaptogenic effects of Panax ginseng on modulation of immune functions. *J Ginseng Res*. 2021;45(1):32–40. doi:10.1016/j.jgr.2020.09.004
24. Chen G, Jiang N, Zheng J, et al. Structural characterization and anti-inflammatory activity of polysaccharides from Astragalus membranaceus. *Int J Biol Macromol*. 2023;241:124386. doi:10.1016/j.ijbiomac.2023.124386
25. Silva BS, Lira FS, Ramos D, et al. Severity of COPD and its relationship with IL-10. *Cytokine*. 2018;106:95–100. doi:10.1016/j.cyto.2017.10.018
26. Yang D, Wang L, Jiang P, Kang R, Xie Y. Correlation between hs-CRP, IL-6, IL-10, ET-1, and chronic obstructive pulmonary disease combined with pulmonary hypertension. *J Healthcare Eng*. 2022;2022(1):3247807. doi:10.1155/2022/3247807

27. Vega G, Guequén A, Philp AR, et al. Lack of Kcnn4 improves mucociliary clearance in muco-obstructive lung disease. *JCI Insight*. 2020;5(16):e140076. doi:10.1172/jci.insight.140076
28. Ran L, Ye T, Erbs E, et al. KCNN4 links PIEZO-dependent mechanotransduction to NLRP3 inflammasome activation. *Sci Immunol*. 2023;8(90):eadf4699. doi:10.1126/sciimmunol.adf4699
29. Thorne A, Bansal A, Necker-Brown A, et al. Differential regulation of BIRC2 and BIRC3 expression by inflammatory cytokines and glucocorticoids in pulmonary epithelial cells. *PLoS One*. 2023;18(6):e0286783. doi:10.1371/journal.pone.0286783
30. Du L, Xu C, Zeng Z, et al. Exploration of induced sputum BIRC3 levels and clinical implications in asthma. *BMC Pulm Med*. 2022;22(1):86. doi:10.1186/s12890-022-01887-2
31. Ma R, Su H, Jiao K, Liu J. Role of Th17 cells, Treg cells, and Th17/Treg imbalance in immune homeostasis disorders in patients with chronic obstructive pulmonary disease. *Immun Inflamm Dis*. 2023;11(2):e784. doi:10.1002/iid3.784
32. Lourenço JD, Ito JT, MdA M. Tibério IdFLC, Lopes FDTQdS. Th17/Treg imbalance in chronic obstructive pulmonary disease: clinical and experimental evidence. *Front Immunol*. 2021;12:804919. doi:10.3389/fimmu.2021.804919
33. Pinzi L, Rastelli G. Molecular docking: shifting paradigms in drug discovery. *Int J Mol Sci*. 2019;20(18):4331. doi:10.3390/ijms20184331
34. Sun X, Chen W, Dai W, et al. Piper sarmentosum Roxb.: a review on its botany, traditional uses, phytochemistry, and pharmacological activities. *J Ethnopharmacol*. 2020;263:112897. doi:10.1016/j.jep.2020.112897
35. Jia Y, He T, Wu D, et al. The treatment of Qibai Pingfei capsule on chronic obstructive pulmonary disease may be mediated by Th17/Treg balance and gut-lung axis microbiota. *J Transl Med*. 2022;20(1):281. doi:10.1186/s12967-022-03481-w
36. Jacobs M, Verschraegen S, Salhi B, et al. IL-10 producing regulatory B cells are decreased in blood from smokers and COPD patients. *Respir Res*. 2022;23(1):287. doi:10.1186/s12931-022-02208-1